Z. Phys C 67, 433–447 (1995)

ZEITSCHRIFT
FÜR PHYSIK C

Dynamical parton distributions of the proton and small-x physics

M. Glück[1], E. Reya[1], A. Vogt[2,★]

[1]Institut für Physik, Universität Dortmund, D-44221 Dortmund, Germany
[2]Deutsches Elektronen-Synchrotron DESY, Notkestrasse 85, D-22603 Hamburg, Germany

Received: 4 January 1995

Abstract. The perturbative properties of parton distributions generated radiatively from a valence-like input at some low resolution scale are discussed with the aim of explaining the physical aspects underlying the reliability of the predicted distributions in the small-x region. Aspects of higher-twist (shadowing) effects as well as small-x resummations are discussed. Utilizing recent improved data at $x \gtrsim 10^{-2}$ and a factorization scheme in which the heavy quarks $c, b, \ldots$, are *not* entailed among the intrinsic (massless) parton distributions, we readjust our valence-like input and provide parametrizations of the slightly modified dynamical LO and NLO ($\overline{MS}$, *DIS*) predictions for parton distributions.

1 Introduction

The original attempt [1] to generate purely dynamically all gluon (g) and sea ($\bar{q} = \bar{u}, \bar{d}, \bar{s}$) distributions merely from measured valence densities was based on the extreme boundary conditions at $Q^2 = \mu^2$ with $\mu = \mathrm{O}(\Lambda)$,

$$g(x, \mu^2) = \bar{q}(x, \mu^2) = 0 \tag{1}$$

in order to avoid any free additional parameters and assumptions in the perturbative renormalization group (RG) evolution to $Q^2 > \mu^2$. This approach works qualitatively well and yields, in particular, the remarkable parameter-free prediction [1] for the momentum fraction carried by gluons, $\int_0^1 xg(x, Q^2)\,dx \simeq 0.45$ at $Q^2 = 1 - 5\,\mathrm{GeV}^2$. Quantitatively, however, the resulting predictions disagree with experiment since the detailed x-dependence of $g(x, Q^2)$ and $\bar{q}(x, Q^2)$ turns out to be much too steep in the small-x region [2, 3] and thus too soft at larger values of x in disagreement with constraints imposed, for example, by the data on direct-photon production.

This purely dynamical approach based on (1) would be indeed physically compelling if the valence distributions $q_v(x, Q^2)$, $q_v \equiv q - \bar{q}$, were identified with the *constituent* quarks in the proton. However, *partonic* quark distributions should rather be identified with the *current* quark content of hadrons. Therefore (1) is not expected to be adequate and is replaced by the assumption that the sea-quarks and gluons follow the valence-quarks [3] at some low resolution scale μ, or more generally [4–6][1]

$$xg(x, \mu^2) = Ax^{\alpha}(1 - x)^{\beta}, \quad x\bar{q}(x, \mu^2) = A'x^{\alpha'}(1 - x)^{\beta'} \tag{2}$$

representing some *valence like* ($\alpha, \alpha' > 0$) structure at $Q = \mu$. Note that the valence-like ansatz is in fact dictated by the obvious *positivity* requirement for the parton distributions down to the low $Q^2 = \mu^2 \simeq (3\Lambda)^2$. Here the gluonic and antiquark (sea) partons are conceived as being frozen upon the valence current quarks[2] (the shapes of their x-dependence, in particular the one of the dominant gluon, turn out to be indeed very similar [4, 5]) at the scale $Q = \mu$ dividing the non-perturbative regime ($Q < \mu$) from the perturbative one ($Q \gtrsim \mu$). They are thus supposed to share the momentum distribution features of the (current!) valence-quark parton distributions.

Experience supports this latter view since the almost unique radiative (dynamical) predictions [4, 5], resulting from the valence-like input in (2), being mainly due to the QCD dynamics and independent of any free (fit) parameters in the small-x region, $x \lesssim 10^{-2}$, seem to be confirmed, for the time being, by all present experimental ep, γp and $\gamma\gamma$ data [8–11]. Due to this, several questions were raised recently (see, for example, the review and summary talks in [12]) concerning the reliability of this somewhat "unbelievable" approach and the reasons for its seeming

★ On leave of absence from Sektion Physik, Universität München, D-80333 Munich, Germany

[1] Due to the gluonic hyperfine interaction ('Z-diagrams' in which gluons connect one quark to another), intrinsic (input) gluon and sea-quark distributions are expected to be always *non*-vanishing [7]. In the next-to-leading order (NLO) (2) was implemented in the $\overline{MS}$ factorization scheme

[2] These stuck-together objects form the constituent quarks!

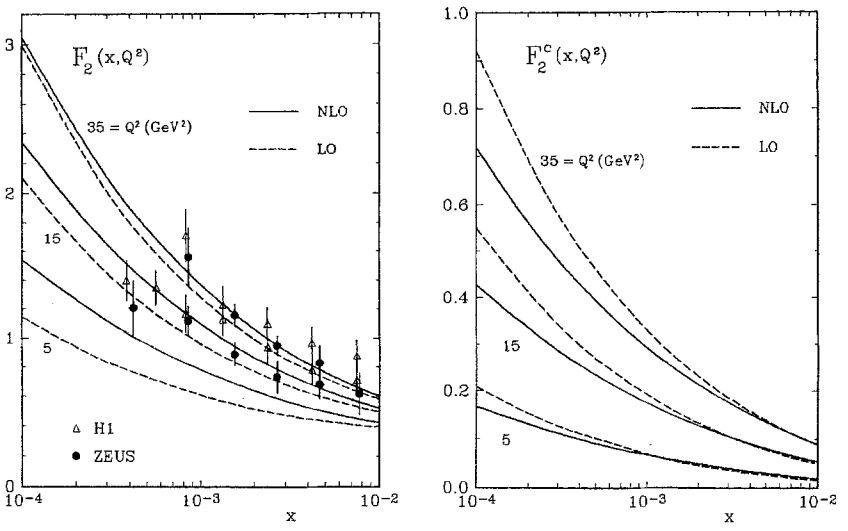

Fig. 1. Representative dynamical LO and NLO GRV predictions [4] for F_2^{ep}. Some recent HERA data [8, 10] are shown as well. The LO and NLO heavy quark (charm) contributions have been calculated via the $\gamma^* g \to c\bar{c}$ and $\gamma^* g$, $\gamma^* q(\bar{q}) \to c\bar{c}X$ fusion subprocesses [15, 16], respectively, using $m_c = 1.5$ GeV. These LO and NLO charm contributions, F_2^c, are shown separately as well

success which we attempt to further clarify in Sect. 2. In Sect. 3 we discuss the implications of some moderate modifications of the valence-like input which are based on improved data at $x \gtrsim 10^{-2}$ but do not significantly affect the (steep) radiative predictions at $x \lesssim 10^{-2}$. This is a continuation and completion of the work started in [3] and generalized to a valence-*like* input in [4], which has been improved in [5], except that now we adopt a factorization scheme in which the heavy quarks ($h = c, b, \ldots$) are *not* included among the massless parton distributions of the nucleon. Finally we present simple analytic parametrizations of the resulting theoretical (dynamical) predictions for the parton distributions in LO and NLO ($\overline{MS}$, *DIS*) in the Appendix.

2 Qualitative properties

As stated in the Introduction we now list the qualitative properties characterizing the radiatively generated ('dynamical') parton distributions based on a valence-like input, as exemplified in (2), and their successful predictions in the small-x region:

(i) *Perturbative reliability.* Since the radiative RG-evolution starts at a low evolution scale $Q = \mu$ with $\mu \simeq 3\Lambda$ (typically $\mu_{LO} \simeq 0.5$ GeV and $\mu_{NLO} \simeq 0.55$ GeV where the gluons and antiquarks in the nucleon are *valence-like* [4, 5]) one may wonder whether a perturbative treatment at such low momentum scales is admissible and reliable. Superficially such an objection is seemingly correct, but so far *no one* really *knows*[3] the range of validity of perturbative QCD. This can be studied, as usual, only by a pragmatic approach trying to find out by methods of trial and error where this perturbative limit actually is. For the present case we find that the perturbative expansion parameters are indeed sufficiently small by comparing the perturbative stability of our predictions in the leading (LO) and next-to-leading (NLO) order. This stability results not only from $\alpha_s(\mu^2)/\pi = 0.2 \ll 1$, but also from the particular shapes of the 1- and 2-loop splitting functions $P_{ij}^{(0)}(x)$ and $P_{ij}^{(1)}(x)$, respectively, as well as from the particular (*different*) shapes of the LO and NLO *input* parton distributions $f(x, \mu^2)$ where $f = q, \bar{q}, g$. These perturbatively stable predictions refer always to *measurable* quantities like $F_2(x, Q^2)$ etc. rather than to the auxiliary, *not directly* measurable, NLO parton distributions $f(x, Q^2)$ as illustrated in Figs. 1 and 2. The 'perturbative instability' of the latter quantities, i.e. $f^{LO}(x, Q^2) \neq f^{NLO}(x, Q^2)$ as exemplified in Fig. 2, should be expected and even tolerated: Despite the sizeable difference of LO and NLO sea and gluon distributions in the small-x region[4] in Fig. 2, the sea ($\bar{u}$) dominated structure function F_2^{ep} in Fig. 1 and its gluon dominated ($\gamma^* g \to c\bar{c}$, etc.) heavy quark contribution F_2^c show a remarkable perturbative stability, which will be even improved in most cases by our slightly modified analysis to be discussed in Sect. 3. A similar (even more pronounced) perturbative NLO stability is also obtained for other directly measurable quantities such as for example F_2^b, $F_L^{c,b}$ ($F_L \equiv F_2 - 2xF_1$), $\sigma(pp \to c\bar{c}X)$ and $\sigma(pp \to b\bar{b}X)$ all the way up to multi-TeV energies [15].

It should, however, be remarked that the (finite) perturbative small-x predictions for $g(x, Q^2)$, $\bar{q}(x, Q^2)$,

[3] Recent lattice calculations of α_s from first principles [13] confirm the perturbative NLO (2-loop) predictions for $\alpha_s(Q^2)$ down to $Q \simeq 0.55\,\text{GeV} \simeq \mu$

[4] It has been speculated [14] that this difference might become even more pronounced if one goes beyond the NLO, using rudimentary (partly guessed) NNLO (α_s^3) and NNNLO(α_s^4) asymptotic ($x \to 0$) expressions for the P_{ij}'s and the *same* input parton distributions at each perturbative order. Apart from this incorrect treatment of the input distributions and the inadequacy of the asymptotic "$1/x$ approximation" for the presently attainable small-x region (see point (v) below), such an approach is likely to be misleading because of our ignorance of *full* NNLO and NNNLO perturbative expressions for *all* splitting functions P_{ij} *as well as* of the corresponding Wilson coefficients. Thus, for the time being, a full perturbative analysis can only be performed up to NLO (α_s^2)

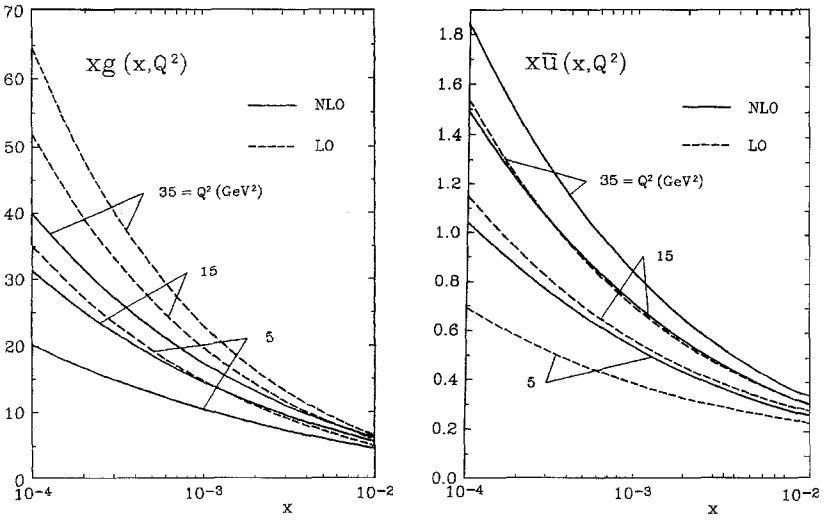

Fig. 2. Dynamical LO and NLO GRV predictions [4] for the light sea ($\bar{u}$) and gluon distributions

$F_i(x, Q^2)$, etc., are strongly varying for Q^2 in the vicinity of $\mu^2_{\text{LO,HO}}$ and thus depend critically on the precise choice of μ^2 which in turn can be fixed, by present experiments, only to within about 10% [5]. Since $Q^2 < \mu^2 \simeq 0.3\ \text{GeV}^2$ refers to the manifestly *non*-perturbative regime, it is not unlikely that also for $Q^2 \simeq \mu^2$ non-perturbative contributions (higher-twists, etc.) remain relevant. Therefore, only well above the valence-like input scale μ, $Q^2 \gtrsim 0.5$–$0.6\ \text{GeV}^2$ say, will our dynamical perturbative predictions become reliable and experimentally relevant.

(ii) *Specific dynamical predictions.* Due to the valence-like structure of the input distributions in (2), our radiative predictions [4] at $Q > \mu$ are rather unambiguous [5], i.e. parameter-*free* in the *small-x* region, $x \lesssim 10^{-2}$. At *larger* scales $Q^2 \gtrsim 5\ \text{GeV}^2$ structure functions like $F_2(x, Q^2)$ and the singlet parton distributions $xg(x, Q^2)$ and $x\bar{q}(x, Q^2)$ are predicted to be *steep* at small-x, as can be seen in Figs. 1 and 2: Typically, at $Q^2 = 10$–$100\ \text{GeV}^2$ F_2, $xg \sim x^{-\lambda}$ with $\lambda_{\text{NLO}} \simeq 0.3$–$0.4$ for $10^{-5} \lesssim x \lesssim 10^{-3}$, i.e. these distributions posses a 'Lipatov'-like ($\lambda \neq 0$) behavior, which has been confirmed by HERA [8, 10]. At *smaller* scales $Q^2 \simeq 1\ \text{GeV}^2$, however, F_2 and xf are predicted to be almost *flat* [4, 5] at small-x, i.e. develop the 'Regge (Pomeron)'-like x-dependence ($\sim x^0$). Although such a trend towards a small-x flattening of $F_2^{\text{ep}}(x, Q^2)$ for decreasing Q^2 is indicated by the recent HERA data [8] as well as [5] by the EMC and NMC data [17], this latter prediction has to be still confirmed by future HERA measurements – it will constitute a fundamental test of the correctness of the radiatively (dynamically) calculated parton distributions.[5] It should be furthermore emphasized that these scale dependent unique small-x *predictions* are not only a consequence of the 'standard' RG evolution equations (due to the large radiative evolution 'distance' $\xi(Q^2) \equiv \ln[\alpha_s(\mu^2)/\alpha_s(Q^2)]$, but follow in particular also from our valence-like gluon and (light) sea content in (2), $xf(x, \mu^2) \to 0$ for $x \to 0$, of the nucleon at a low resolution scale[6] $\mu \simeq 3\Lambda$. Both ingredients, as well as the specific shapes of the perturbatively calculable splitting functions $\mathrm{P}_{ij}^{(0,1)}(x)$ and of the Wilson-expansion coefficients, seem to provide the correct small-x behavior of $F_2(x, Q^2)$ as measured at HERA [8, 10]. (Here *no* further assumptions or small-x extrapolations of $f(x, Q_0^2)$ at, say, $Q_0^2 = 4\ \text{GeV}^2$ – usually implemented in all alternative, mainly fit-inspired, parametrizations of parton distributions [18, 20] – are needed or employed.)

(iii) *Higher-twist* ('*shadowing*') *effects.* At the low scales $Q \gtrsim \mu$ higher-twist $\tau > 2$ effects, suppressed by powers of $1/Q^{\tau-2}$, might a priori become quite important, as compared with the dominant twist $\tau \equiv$ dimension $-$ spin $= 2$ effects considered thus far. Here one should clearly distinguish between two different matters: (a) the possible higher-twist contributions to measurable quantities like $F_2(x, Q^2)$ and (b) their strict *decoupling*[7] from the underlying Q^2-evolution equations for the standard *covariant* twist-2 parton distributions $f(x, Q^2)$ utilized in all our subsequent physical applications.[8] Covariantly defined

[5] It should be noted that such tests are not feasible for the alternative standard fits of parton distributions where an ansatz for the input distributions $xf(x, Q_0^2)$ with an assumed (flat or steep) small-x behavior is fitted to the data at $Q_0^2 = 4\ \text{GeV}^2$ for example (see, e.g., [18]). In this case the highly unstable 'backward' evolution to $Q^2 < Q_0^2$ would lead to negative parton distributions [19]

[6] Note that there is only one scale μ where such a valence-like structure can exist, which is fixed by experiment in order to obtain a large enough amount [4, 5] of $\bar{q}(x, Q^2)$ and $g(x, Q^2)$ at $Q^2 > \mu^2$ (and $x \gtrsim 0.01$). Present experimental uncertainties would allow our $\mu_{\text{HO}} \simeq 0.55\ \text{GeV}$ to be increased by at most about 10%[5]

[7] This is essential for obtaining universal, i.e. process *in*dependent parton distributions $f(x, Q^2)$ which can be used for studying any other hard scattering process - the main virtue of the entire fundamental concept of the parton model

[8] Strictly speaking our structure functions and parton distributions should be expressed in terms of the ξ-scaling variable [21], instead of the Bjorken-x. This becomes particularly relevant in the low-Q^2 region and at large x where, among other things, higher-twist contributions are essential [21] also for satisfying the energy threshold constraints. In the small-x region such subtleties are of no importance

operators of different twists do *not* mix under renormalization! This should be distinguished from approaches [22, 23] referring to k_T-cutoff regulated 'parton distributions' $\tilde{f}(x, Q^2)$ which, being *non-covariant*, may mix with higher-twist-like distributions[9] leading to possible "shadowing" (or "screening") effects of the non-standard "twist-2" $\tilde{f}(x, Q^2)$ in the low-x region. Here these nonlinear shadowing effects ($\sim -C/R^2Q^2$ with R being the proton radius, $R \simeq 5\,\mathrm{GeV}^{-1}$, or a smaller 'hot-spot' screening parameter, $R \simeq 2\,\mathrm{GeV}^{-1}$) cause a flattening of originally steep input distributions $x\tilde{f}(x, Q_0^2)$ in the small-x region. The recent steep HERA results [8, 10] apparently do not support this approach. (It is interesting to note that, prior to HERA measurements, it has been anticipated [25] that a consistent treatment of the nonlinear GLR-equations [22, 23] leaves little room for shadowing effects in the kinematic region attainable by HERA, provided structure functions are steep in the small-x region at a typical input scale of $Q^2 \simeq 4\,\mathrm{GeV}^2$.)

Shadowing-like effects appear in our standard covariant twist-diagonal approach merely via the chosen valence-like input $xf(x, \mu^2)$ in (2) as well as due to the particular influence of the two-loop splitting functions $P_{ij}^{(1)}(x)$ in the NLO evolution which reduce [4] the naive LO results in the small-x region.[10] The remaining possible influence of higher-twist contributions on, say, $F_2(x, Q^2)$ at low Q^2 can only be inferred phenomenologically: Comparing our predicted results for $F_2(x, Q^2)$ with, say, the EMC-NA28, NMC and SLAC μ(e)d data we note [4, 5] that higher-twist contributions at $x \lesssim 0.01$ are at most marginal even at $Q^2 \lesssim 1\,\mathrm{GeV}^2$, as long as $Q^2 > \mu_{\mathrm{HO}}^2 \simeq 0.3\,\mathrm{GeV}^2$ (cf. Fig. 11 below). On the other hand, nonperturbative effects, as eventually also required by unitarity, will be essential for $Q^2 \lesssim \mu^2$, since in the photoproduction limit, $F_2(x, Q^2 \to 0) \to 0$ is *not* reproducible within a perturbative parton model.

(iv) *No strong k_T-ordering in ladder summations, i.e. in Q^2-evolutions.* The leading logarithms resummed by the Altarelli-Parisi RG evolution equations at the LO correspond to a summation of quark and gluon ladders with strongly ordered transverse momenta in the n rungs ($Q^2 > k_{nT}^2 > \cdots > k_{1T}^2 > Q_0^2$). For small x but moderate Q^2 this simple and naive LO approach is expected to break down since ladder contributions with no strong k_T-ordering will obviously become important and one clearly has to integrate over the full k_T phase space [26, 22]. Such contributions have been formulated (BFKL summation) and calculated just for gluon ladders in the LO resulting in a steeper small-x 'Lipatov'-like gluon distribution $xg \sim x^{-\lambda}$ with $\lambda \leq \lambda_{\max} = (3\alpha_s/\pi)4\ln 2 \simeq 0.5$ as already referred to in (ii). Unfortunately the *detailed* BFKL results strongly depend on the specific choice of the various infrared k_T-cutoffs required for explicit calculations [27] and thus carry little overall predictive power. They furthermore only represent the LO 'asymptotic' small-x behavior of the gluon distribution.[11] It is thus certainly true that the LO Q^2-evolution based on $P_{ij}^{(0)}(x)$ becomes unreliable in the small x-region due to the summation of just strongly k_T-ordered ladders, but *non*-ordered k_T ladder contributions are involved as soon as NLO Q^2-evolutions, containing the two-loop $P_{ij}^{(1)}(x)$, are considered. These, moreover, are treated in a strictly covariant way in contrast to the k_T-regularized distributions $\tilde{f}(x, Q^2)$ in [22, 23, 26] which, as mentioned before in (*iii*), should not be directly compared with our strictly covariantly evolved $f(x, Q^2)$.

(v) *Resummations of small-x singularities of splitting functions?* It has been frequently claimed [29, 14] that the singular behavior of $P_{ij}^{(0)}(x)$ and $P_{ij}^{(1)}(x)$ in the small-x region requires a resummation of leading small-x singularities in

$$P_{ij}(x, Q^2) = \frac{\alpha_s(Q^2)}{2\pi} P_{ij}^{(0)}(x) + \left(\frac{\alpha_s(Q^2)}{2\pi}\right)^2 P_{ij}^{(1)}(x) + \ldots \quad (3)$$

before performing any (reliable) Q^2-evolution analysis in the small-x region. However, as noted recently [15], this seemingly alarming danger disappears as soon as one recognizes that the P_{ij}'s always appear in the Q^2-evolution equations convoluted with some very specific parton distribution functions and that the question of the low-x perturbative stability of the investigated Q^2-evolutions crucially depends on the *particular* shapes of the involved LO and NLO parton distributions. As already noted in (i) our particular radiatively generated LO and NLO parton distributions do not give rise to physically relevant perturbative instabilities for directly measurable quantities in the small-x region despite of the noted [29, 14] bad convergence of $P_{ij}(x, Q^2)$ itself as $x \to 0$.[4] This implies in particular also that one has *always* to perform a *full* NLO analysis (i.e. to keep the full $P_{ij}^{(n)}(x)$ *and* the appropriate Wilson coefficients) for obtaining perturbatively relevant and reliable results. Recent studies of NLO and NNLO contributions [30] have explicitly demonstrated that the "$1/x$ approximation", used in most small-x studies [14, 23, 26, 29], is insufficient even down to $x = 10^{-5}$ and thus that resummations of $1/x$ and $\ln x/x$ terms are not very useful and even misleading. This further demonstrates the care needed before making any *general* statements concerning perturbative stability [14, 29], nonphysical small-x behavior [22, 26], etc.

(vi) *Possible implications for lattice calculations.* It is more than surprising that the 'quenched' or 'valence' approximation, where the effect of virtual $q\bar{q}$-excitations on the lattice is ignored for technical reasons, works that well in describing the observed hadron mass spectra (for a recent review, see [31]). It is tempting to speculate that our dynamical valence-like parton model [3–5] offers some rationale for this success since at a length scale

[9] The twist concept is unambiguously defined only in *covariant* formulations of deep inelastic scattering which requires fermionic and gluonic Wilson operators of definite spin (i.e. traceless) and dimension (see, for example [24] and the appropriate discussion on pp. 442, 443 of [23]

[10] This should also apply to nuclear shadowing still to be studied within our dynamical approach

[11] It is difficult to envisage how the conceptionally important NLO contributions, which are essential for establishing the reliability of the LO BFKL-results, can be calculated within the non-covariant k_T-cutoff regulated ladder approach [28]

$\mu^{-1} \simeq (0.55\,\text{GeV})^{-1} \simeq 0.5\,\text{fm}$ the proton consists dominantly of valence quarks and valence-like gluons, i.e. with only about 10% $q\bar{q}$-excitations (sea quarks). The latter become important only at perturbative length scales less than μ^{-1} but appear to be *negligible* at scales larger than $\mu^{-1} \simeq 0.5\,\text{fm}$ typical for lattice calculations. It would be interesting to see whether the non-perturbative valence-like distributions at $Q^2 = \mu^2$, which we have determined purely phenomenologically, can be obtained, in some forthcoming lattice QCD analysis, from first principles.

(vii) *Universality*. Finally we emphasize the universal character of our radiative (dynamical) valence-like parton model approach which allows for its application also to other objects such as the pion [32] and the photon [33][12] where it enables one to explore the almost unknown photonic gluon distribution $g^\gamma(x, Q^2)$. These predictions seem to lie in the right ball park of preliminary LEP, TRISTAN (e^+e^-) and HERA (ep) measurements [9–11].[13] Furthermore the dynamical radiative concept also provides us with access to the time-like region ($Q^2 \equiv -q^2 < 0$), e.g. for analyzing the fragmentation functions of partons into photons [34] which have so far, however, not been measured but play a crucial role in understanding and explaining prompt photon rates at small to medium values of p_T^γ as observed at high energy $p\bar{p}$ colliders [35].

3 Improved quantitative results

As exemplified in Fig. 1 the small-x predictions of our radiative (dynamical) parton distributions [4, 5], derived from valence-like input densities, are confirmed by recent HERA measurements [8, 10], in particular if the LO and NLO heavy quark (charm) contributions are calculated via the $\gamma^* g \to c\bar{c}$ and $\gamma^* g \to c\bar{c}g$, $\gamma^* q(\bar{q}) \to c\bar{c}q(\bar{q})$ fusion subprocesses [15, 16]. Moreover, according to the conclusions of [15], a consistent and perturbatively stable treatment of heavy flavor contributions affords a choice of a factorization scheme in which the heavy quarks ($h = c, b \ldots$) are *not* considered as (intrinsic) partons in the nucleon, but are treated in fixed-order perturbation theory as specified above, i.e. being produced via the intrinsic gluon and $f = 3$ light flavor quarks (u, d, s) of the nucleon. Thus, in contrast to the conventional $\overline{\text{MS}}$ treatment [3–5, 18, 20] where 'heavy' quark distributions $h(x, Q^2) = \bar{h}(x, Q^2)$ are radiatively generated using the massless evolution equations for $Q^2 \geq m_h^2$, we now *fix* the number of flavors entering the splitting functions in (3), or more specifically in (2.3) and (2.4) of [3], to be $f = 3$ and refrain from generating massless 'heavy' flavor distributions $h(x, Q^2)$. We consider this approach more realistic and reliable than the purely massless treatment of 'heavy' quark distributions. Our renormalization scheme for the running coupling constant $\alpha_s(Q^2)$ will, however, be kept unchanged, i.e. *including* the contributions from heavy virtual quark flavors to the β-function and the related matching conditions for $\Lambda^{(f)}$ [3] at each 'threshold' $Q = m_h$ as required by the continuity of $\alpha_s(Q^2)$.[14]

The second element entering our improved quantitative results concerns minor modifications [5] of the valence-like input at $x > 10^{-2}$ as indicated by the NMC and BCDMS data [17, 36, 37] as well as a modification of the $\bar{u} = \bar{d}$ symmetry indicated [17, 36] by the violation of the Gottfried sum rule for $F_2^p - F_2^n$ and established by the Drell-Yan dilepton production measurements in pp and pd collisions of the NA51 collaboration [38]. Here we adopt the 'valence-like' parametrization of the MRS(A) fit [18] for $\Delta \equiv \bar{d} - \bar{u}$ at $Q^2 = 4\,\text{GeV}^2$. Finally, the low input scale μ^2 of the valence-like input distributions in (2) which according to [3–5] has to be optimized according to the data at $x \gtrsim 10^{-2}$ was slightly changed in LO and NLO as compared to [4, 5] so as to provide an even better agreement with the recent small-x ($< 10^{-2}$) results of the H1 and ZEUS collaboration at HERA [8].[15] These latter modifications of μ_{LO}^2 and μ_{HO}^2 are only at the 10% level [5] and do not affect our main observation in [4, 5] that the predictions of the radiative (dynamical) parton distributions in the small-x region, being mainly due to the QCD dynamics, are remarkably stable at $x \lesssim 10^{-2}$.

The required valence and valence-like input distributions at $Q^2 = \mu^2$ have been fixed as follows: For definiteness we have adopted the recent set of NLO($\overline{\text{MS}}$) non-singlet distributions, $u_v \equiv u - \bar{u}$, $d_v \equiv d - \bar{d}$ and $\Delta \equiv \bar{d}$-$\bar{u}$, as obtained by the MRS(A) fit [18] at $Q^2 = 4\,\text{GeV}^2$. For our LO calculation we have derived corresponding distributions by demanding the same non-singlet (u_v, d_v, Δ) contributions to $F_2^{p,n}$ within $0.003 \leq x \leq 0.9$. For the appropriate evolutions we used the $\Lambda^{(f)}$ values as specified below (eq. (11)). The LO and NLO valence-like gluon and sea input distributions have been obtained by using a simple ansatz, similar to the one in (2), with the parameters fitted to the NMC [17], BCDMS [37], (renormalized, as usual, by a factor 0.98) and SLAC [39] $F_2^{p,d}$ data at $x < 0.3$ and $Q^2 \geq 5\,\text{GeV}^2$ where of

[12] In NLO the valence-like hadronic VMD input was implemented in a specific factorization scheme (DIS_γ) chosen so as to minimize NLO corrections to measurable quantities such as $F_2^\gamma(x, Q^2)$, etc. This factorization scheme amounts to choosing a vanishing photonic Wilson coefficient, which contributes in NLO to F_2^γ, while keeping the partonic Wilson coefficients in the $\overline{MS}$ factorization scheme as in the corresponding hadronic case discussed so far

[13] Obviously there are inherent uncertainties due to the hadronic valence-like vector-meson-dominance input at $Q^2 = \mu^2$ which, however, do not significantly affect our small-x predictions as in the corresponding case of the nucleon

[14] Although this matching of $\alpha_s(Q^2)$ is important for the LO and NLO evolutions of the light ($u, d, s; g$) parton distributions, their resulting x- and Q^2-dependence is not very sensitive to whether $h(x, Q^2)$, $h = c, b, \ldots$, is included [3–5, 18, 20] in their evolutions or not. In particular the results or physical quantities ($F_{1,2,L}(x, Q^2)$, cross sections, etc.) remain practically unaltered

[15] These modifications improve also the perturbative stability of the LO and NLO predictions for F_2, etc.. Note that perturbative stability is mainly afforded for *physical* quantities like F_2 but not for the (auxiliary) parton distributions $f(x, Q^2)$, as has been discussed in detail in Sect. 2(i)

course the appropriate LO and NLO Q^2-evolutions [3][16] have been taken into account. The gluon distribution at larger values of x, $g(x \geq 0.25, Q^2)$, has been constrained by the direct-photon results [40] as in our previous analysis [4, 5]. These parameters, in particular the ones of the gluon density, are furthermore constrained by the energy-momentum conservation relation

$$\int_0^1 x[u_v(x,\mu^2) + d_v(x,\mu^2) + 2\bar{u}(x,\mu^2) + 2\bar{d}(x,\mu^2) + g(x,\mu^2)]\,dx = 1 \tag{4}$$

for the following input distributions. The resulting LO input at $Q^2 = \mu^2_{LO} = 0.23\ \text{GeV}^2$ is then given by

$$\begin{aligned}
xu_v(x,\mu^2_{LO}) &= 1.377\,x^{0.549}(1 + 0.81\sqrt{x} - 4.36x \\
&\quad + 19.4x^{3/2})(1-x)^{3.027} \\
xd_v(x,\mu^2_{LO}) &= 0.328\,x^{0.366}(1 + 1.14\sqrt{x} + 5.71x \\
&\quad + 16.9x^{3/2})(1-x)^{3.774} \\
x\Delta(x,\mu^2_{LO}) &= 0.0697\,x^{0.397}(1 + 5.0x + 92x^{3/2})(1-x)^{7.88} \\
x(\bar{u}+\bar{d})(x,\mu^2_{LO}) &= 1.20x^{0.29}(1 + 0.31x)(1-x)^{7.03} \\
xg(x,\mu^2_{LO}) &= 35.8x^{2.3}(1-x)^{4.0} \\
s(x,\mu^2_{LO}) &= \bar{s}(x,\mu^2_{LO}) = 0
\end{aligned} \tag{5}$$

with $\Delta \equiv \bar{d} - \bar{u}$. The corresponding NLO input in the $\overline{MS}$ factorization scheme at $Q^2 = \mu^2_{HO} = 0.34\ \text{GeV}^2$ is

$$\begin{aligned}
xu_v(x,\mu^2_{HO}) &= 0.988\,x^{0.543}(1 + 1.58\sqrt{x} + 2.58x \\
&\quad + 18.1x^{3/2})(1-x)^{3.380} \\
xd_v(x,\mu^2_{HO}) &= 0.182\,x^{0.316}(1 + 2.51\sqrt{x} + 25.0x \\
&\quad + 11.4x^{3/2})(1-x)^{4.113} \\
x\Delta(x,\mu^2_{HO}) &= 0.0525\,x^{0.381}(1 + 15.2x + 132x^{3/2})(1-x)^{8.65} \\
x(\bar{u}+\bar{d})(x,\mu^2_{HO}) &= 1.09x^{0.30}(1 + 2.65x)(1-x)^{8.33} \\
xg(x,\mu^2_{HO}) &= 26.2x^{1.9}(1-x)^{4.0} \\
s(x,\mu^2_{HO}) &= \bar{s}(x,\mu^2_{HO}) = 0.
\end{aligned} \tag{6}$$

It should be noted that we have assumed a vanishing strange sea at the input scale μ in order to comply with experimental indications [44, 45] of an SU(3)-broken sea as well as with recent measurements [45] of $s(x, Q^2 > \mu^2)$, which is thus generated purely dynamically (radiatively) and therefore constitutes an absolute, i.e. parameter-free prediction. It should, however, be kept in mind that future precision experiments might very well require a finite, valence-like, strange sea input at $Q^2 = \mu^2$ as is the case for the $\bar{u}$ and $\bar{d}$ distributions.

The resulting LO and NLO parton distributions $(u, d, s; g)$, as parametrized in the Appendix,[17] are then directly related to the physical quantities such as structure functions where the NLO($\overline{MS}$) distributions have obviously always to be used in conjunction with the corresponding NLO cross sections, i.e. Wilson coefficients, calculated in the $\overline{MS}$ scheme:

$$\begin{aligned}
\frac{1}{x}F_2^{ep}(x,Q^2) &= \sum_q e_q^2 \Big\{ q(x,Q^2) + \bar{q}(x,Q^2) + \frac{\alpha_s(Q^2)}{2\pi} \\
&\quad \times \Big[C_{q,2} * (q + \bar{q}) + 2C_{g,2} * g \Big] \Big\} \\
&\quad + \frac{1}{x}F_2^c(x,Q^2,m_c^2)
\end{aligned} \tag{7}$$

with

$$\begin{aligned}
C_{q,2}(z) &= \frac{4}{3}\left[\frac{1+z^2}{1-z}\left(\ln\frac{1-z}{z} - \frac{3}{4} \right) + \frac{1}{4}(9+5z) \right]_+ \\
C_{g,2}(z) &= \frac{1}{2}\left[(z^2 + (1-z)^2)\ln\frac{1-z}{z} - 1 + 8z(1-z) \right]
\end{aligned} \tag{8}$$

and the sum extends over all light quarks $q = u, d, s$. The convolutions are defined as usual

$$C * q = \int_x^1 \frac{dy}{y} C\left(\frac{x}{y}\right) q(y, Q^2) \tag{9}$$

and the convolution with the $[\,]_+$ distribution in (8) can be easily calculated using, for example, (A.21) of [4]. Finally

$$\frac{\alpha_s(Q^2)}{2\pi} = \frac{2}{\beta_0 \ln(Q^2/\Lambda^2)} - \frac{2\beta_1}{\beta_0^3}\frac{\ln\ln(Q^2/\Lambda^2)}{[\ln(Q^2/\Lambda^2)]^2} \tag{10}$$

with $\beta_0 = 11 - 2f/3$ and $\beta_1 = 102 - 38f/3$. The LO expressions are obviously entailed in the above equations by simply dropping all higher order terms $(C_{i,2}, \beta_i)$ in (7) and (10). Furthermore we choose [46] $\Lambda^{(f=4)}_{LO} = \Lambda^{(4)}_{\overline{MS}} = 200$ MeV to conform with our previous analyses of nucleonic, pionic and photonic parton distributions [4, 5, 32, 33] as well as fragmentation functions [34]. The matching of $\alpha_s(Q^2)$ at each 'threshold' $Q = m_h$,

[16] It should be pointed out that we have (analytically) calculated all Q^2-evolutions in Mellin n-moment space [3], which can be easily Mellin-inverted numerically [3] for obtaining the parton distributions and structure functions in Bjorken-x space. Similar numerical inversion techniques have been used previously [2, 41], following the work in [42] which was carried further in [43]. The advantage of using the Mellin-inversion method is that it allows, among other things, for explicit analytical solutions of the LO and NLO evolution equations which implies that for obtaining the results in x-space, only a single numerical integration is required. This is in contrast to the alternative method of iteratively solving the integro differential evolution equations directly in Bjorken-x space, and is particularly advantageous for calculating photonic parton distributions [33]. All details for practical LO and NLO inversions, as well as the required analytic continuations in n of the moments of splitting functions and Wilson coefficients can be found in [3]

[17] For situations, where the appropriate massive (NLO) subprocesses have not been calculated, a rough estimate (valid to within a factor of 2 to 3, say) of production rates involving heavy quarks $(c, b, \ldots)$ can be obtained with the help of the massless 'heavy' quark distributions $c(x,Q^2)$ and $b(x,Q^2)$ given in [4], for example

$h = c, b, \ldots$, encountered in the Q^2-evolutions, results in [4]

$$\Lambda_{\overline{\rm LO}}^{(3,4,5)} = 232{,}200{,}153\ \text{MeV}$$

$$\Lambda_{\overline{MS}}^{(3,4,5)} = 248{,}200{,}131\ \text{MeV}. \tag{11}$$

As has been discussed at the beginning of this section, a consistent and perturbatively stable treatment of the heavy flavor contribution F_2^c in (7) (we keep only the dominant charm contribution since the bottom one is marginal) is provided by fixed-order perturbation theory, according to the conclusions of [15]. Thus, for $W^2 \equiv Q^2(1/x - 1) \geq (2m_c)^2$, in LO

$$\frac{1}{x} F_2^c(x, Q^2, m_c^2) = 2e_c^2 \frac{\alpha_s(\mu'^2)}{2\pi} \int_{ax}^{1} \frac{dy}{y} C_{g,2}^c\left(\frac{x}{y}, \frac{m_c^2}{Q^2}\right) g(y, \mu'^2) \tag{12}$$

with $a = 1 + 4m_c^2/Q^2$ and the LO fusion process $\gamma^* g \to c\bar{c}$ gives

$$C_{g,2}^c\left(z, \frac{m_c^2}{Q^2}\right) = \frac{1}{2}\left\{\left[z^2 + (1-z)^2 + z(1-3z)\frac{4m_c^2}{Q^2} - z^2\frac{8m_c^4}{Q^4}\right] \times \ln\frac{1+\beta}{1-\beta} + \beta\left[-1 + 8z(1-z) - z(1-z)\frac{4m_c^2}{Q^2}\right]\right\} \tag{13}$$

where $\beta^2 = 1 - (4m_c^2/Q^2)z(1-z)^{-1}$. The factorization scale μ' should be preferrably $\mu'^2 = 4m_c^2$, irrespective of Q^2, which results in a satisfactory perturbative stability when compared with the appropriate NLO contribution [15]. For definiteness we use $m_c = 1.5$ GeV. The NLO($\overline{\rm MS}$) contribution to F_2^c has been calculated recently [16] and, for the time being, its quantitative evaluation is very cumbersome and time-consuming. It turned out, however, that numerically it is close [15] to the LO result in (12), although slightly smaller, in the kinematic region relevant for HERA. We therefore suggest, for any practical purpose, to use the much simpler LO result in (12) also for a NLO analysis of $F_2^{\rm ep}$, as long as a numerically less complicated version of the NLO cross sections in [16] is not available. This represents a sufficiently accurate description of the charm contribution to the total $F_2^{\rm ep}$ in (7). We shall use the simple LO expression (12), utilizing of course α_s and g in LO, also for our NLO analysis from now on.

Similarly, the longitudinal structure function $F_L \equiv F_2 - 2xF_1$ is given by

$$\frac{1}{x} F_L^{\rm ep}(x, Q^2) = \frac{\alpha_s(Q^2)}{2\pi} \sum_q e_q^2 [C_{q,L}^* (q + \bar{q}) + 2C_{g,L}^* g] + \frac{1}{x} F_L^c(x, Q^2, m_c^2) \tag{14}$$

with the convolutions being defined in (9) and

$$C_{q,L}(z) = \frac{8}{3} z, \quad C_{g,L}(z) = 2z(1-z). \tag{15}$$

Equation (14) refers to a NLO expression since the NLO coefficient functions are defined and obtained via $C_L \equiv C_2 - 2C_1$. (It should be noted that in LO $F_L(x, Q^2)$ vanishes (Callan-Gross relation) up to heavy quark corrections stemming from the LO fusion subprocess $\gamma^* g \to h\bar{h}$ [15].) Therefore, the charm contribution in (14) should, for consistency, also be calculated in the NLO [15, 16]. Again it turns out that the much simpler LO expression ($\gamma^* g \to c\bar{c}$) is quantitatively very similar to the far more complicated NLO one in the kinematic HERA region [15]. Hence we suggest to use, for practical purposes, just the LO expression for $F_L^c(x, Q^2, m_c^2)$ in (14) which is formally identical to the LO expression in (12) but with

$$C_{g,L}^c\left(z, \frac{m_c^2}{Q^2}\right) = -z^2 \frac{4m_c^2}{Q^2} \ln\frac{1+\beta}{1-\beta} + 2\beta z(1-z). \tag{16}$$

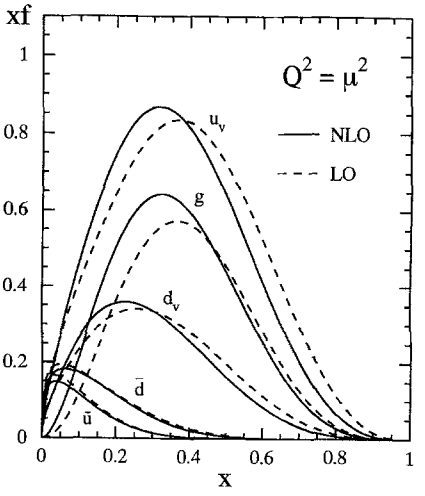

Fig. 3. The valence-like input distributions xf ($f = u_v, d_v, \bar{u}, \bar{d}, g$) at $Q^2 = \mu_{\rm LO}^2 = 0.23$ GeV^2 and $Q^2 = \mu_{\rm HO}^2 = 0.34$ GeV^2 for our LO and NLO calculations. The strange sea $s = \bar{s}$ vanishes at the input scale $Q^2 = \mu^2$

The valence-like gluon- and sea-input and the valence-input distributions at $Q^2 = \mu^2$ for the LO and NLO evolutions are shown in Fig. 3. It is perhaps worthwhile to mention that the large-x behavior of gluon distributions as derived in [7] happens to coincide with our input $g(x, \mu^2) \sim (1-x)^4$, eqs. (5) and (6), as determined from direct-γ results. It is instructive to follow first the Q^2-evolution of the total momentum fractions $\int_0^1 x f(x, Q^2)\, dx$ carried by quarks and gluons as shown in fig. 4. The perturbative stability of the LO and NLO results down to $Q^2 \simeq 0.3$ GeV^2 is remarkable. Although our gluon distributions in (5) and (6), as shown in Fig. 3, carry about 30% of the nucleon's momentum at $Q^2 = \mu_{\rm LO,HO}^2$, $\int_0^1 x g(x, \mu_{\rm LO}^2) dx = 0.25$ and $\int_0^1 x g(x, \mu_{\rm HO}^2) dx = 0.28$, they quickly reach about 50% for $Q^2 \gtrsim 5$ GeV^2 as experimentally required. Similarly, although we start with a vanishing strange quark input, the strange sea ($2\bar{s}$) carries already about 3% of the momentum at $Q^2 \simeq 10$ GeV^2 according to Fig. 4 in LO and NLO, in agreement [4] with measured values [44, 45]. The x-dependence of our NLO parton distributions at $Q^2 = 10$ GeV^2, in particular the typical radiative small-x predictions, are shown in Fig. 5 and compared with the latest MRS(A) fit [18]. Note that our strange quark distribution becomes similar to the

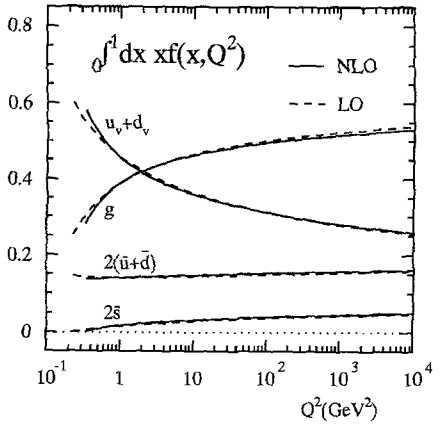

Fig. 4. The predicted Q^2-evolutions of the LO and NLO total momentum fractions of $f = u_v + d_v$, g, $2(\bar{u} + \bar{d})$, $2\bar{s}$

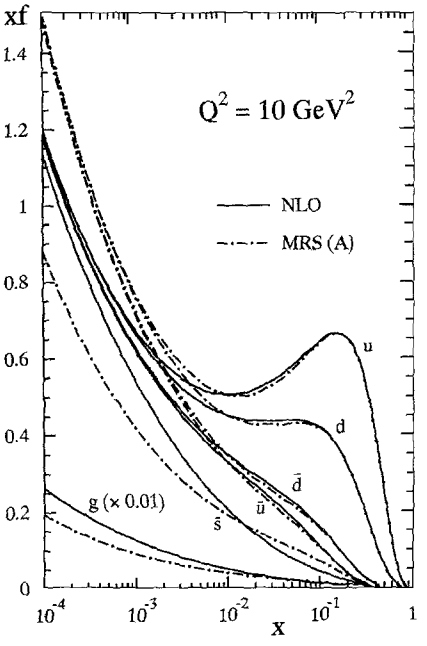

Fig. 5. A comparison at $Q^2 = 10\ GeV^2$ of the radiatively generated parton distributions and the MRS(A) set of partons [18]. The results for the gluon have been multiplied by 0.01

light sea at small-x, $s(x,Q^2) \simeq \bar{u}(x,Q^2)$, which is in contrast to MRS(A) where the input at $Q_0^2 = 4\ GeV^2$ has been constrained by $2s/(\bar{u}+\bar{d}) = 0.5$. Because of the long evolution 'distance' $\xi(Q^2)$, this is a typical input-independent prediction of our dynamical approach. As mentioned already at the beginning of this Section, the symmetry breaking of the light sea, $\bar{d} > \bar{u}$, complies [18] with the Gottfried sum rule for $F_2^p - F_2^n$ [36] as well as with the requirements from the asymmetry measurements [38] of Drell-Yan dilepton production in pp and pd collisions, i.e. $\bar{u}/\bar{d} \simeq 0.56$ at $x = 0.18$ and $Q^2 \simeq 30\ GeV^2$. Furthermore, our LO and NLO u and d distributions (at $Q^2 = M_w^2$) result in predictions [47][18] for the $W^{\pm}$ charge asymmetry, or more precisely for the asymmetry $A(y_l)$ of the charged lepton from the $W^{\pm}$ decay with rapidity y_l produced in $p\bar{p}$ collisions,

$$A(y_l) = \frac{d\sigma(l^+)/dy_l - d\sigma(l^-)/dy_l}{d\sigma(l^+)/dy_l + d\sigma(l^-)/dy_l}, \tag{17}$$

which are in excellent agreement with Fermilab measurements [49]. A similarly good agreement is obtained with our previous ($\bar{u} = \bar{d}$) dynamical LO and NLO distributions [4, 5].[19]

The typically steep radiative (dynamical) small-x LO and NLO predictions for the gluon and sea ($\bar{u}$) distributions are shown in Figs. 6 and 7, for representative values of Q^2, where they are also compared with MRS(A) parametrization [18]. A comparison with our previous results [4, 5], as illustrated in Fig. 2, shows that the present predictions are changed by less than 10% which is mainly due to [5] the slightly different LO and NLO input scales μ_{LO}^2 and μ_{HO}^2 in (5) and (6). The effective slopes $\lambda_f(x,Q^2)$ for $x \ll 1$,

$$xf(x,Q^2) \sim x^{-\lambda_f(x,Q^2)}, \tag{18}$$

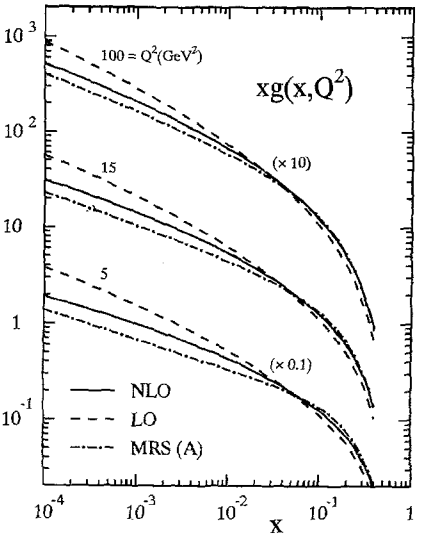

Fig. 6. The predicted small-x behavior of our radiatively generated gluon distributions in LO and NLO. For comparison we also show the MRS(A) gluon density [18]. The results are multiplied by the numbers indicated

as predicted in Figs. 6 and 7, are shown separately in Fig. 8 as a function of Q^2 for three fixed values of x. This figure nicely illustrates the typical feature of the unambiguous dynamical small-x predictions which are steep ($\lambda_f > 0$) at large values of Q^2, whereas for decreasing values of Q^2 they become flatter ($\lambda_f \to 0$) as can be directly observed in $F_2(x,Q^2)$. This latter feature is illustrated in Fig. 9 where, for comparison, we also show our previous not too different LO and NLO results [4, 5]. It should be noted, in particular, that the perturbative

[18] We thank Nigel Glover for providing us with the NLO DYRAD program [48]. Furthermore we thank him as well as S. Kretzer and M. Stratmann for their cooperation in calculating the NLO W-asymmetry

[19] It should be noted that the calculations for $A(y_l)$ presented in [49] for the GRV-NLO distributions are incorrect, being generally too large [47]

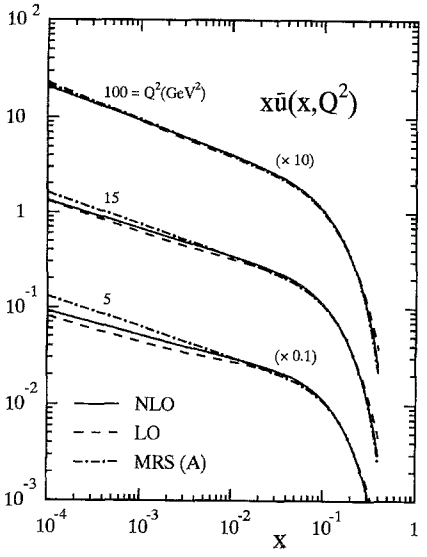

Fig. 7. The same as in Fig. 6 but for the sea distribution $x\bar{u}$

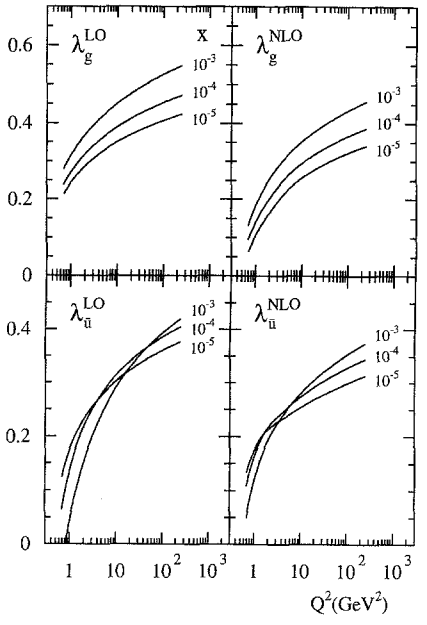

Fig. 8. Dynamical predictions for the effective slopes $\lambda_f(x, Q^2)$ at small-x as defined in (18) for $f = \bar{u}, g$

stability of the experimentally observable $F_2(x, Q^2)$ is considerably improved throughout the kinematic region relevant for HERA measurements, as compared to our previous LO and NLO predictions [4, 5].

In Fig. 10 we compare our fitted LO and NLO results with the NMC, BCDMS and SLAC fixed-target data [17, 37, 39] for F_2^p (the agreement with F_2^d is equally good) where we show only the kinematic region which has been used to determine our valence-like gluon and sea $(\bar{u} + \bar{d})$ input distributions at $Q^2 = \mu^2_{\mathrm{LO,HO}}$ as given in (5) and (6). In Fig. 11 our resulting leading twist predictions in the small-x region ($x < 0.05$) are then compared with the NMC [17] and the preliminary Fermilab E665 [50] data where the latter have been renormalized by a factor of 1.2

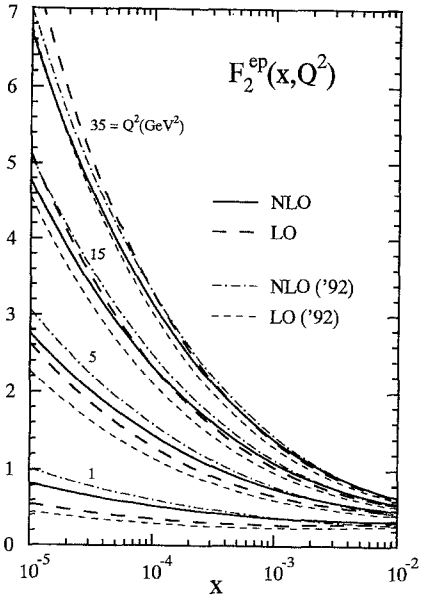

Fig. 9. Radiative LO and NLO small-x predictions for $F_2^{ep}(x, Q^2)$. For comparison we also show the results of our previous LO('92) and NLO('92) analysis [4, 5]. The (heavy) charm contribution has always been calculated according to (12) as discussed in the text. The marginal bottom-quark contribution to F_2 has been neglected

taking into account their present systematic uncertainty [50]. It should be noted that in the small-Q^2 region for $x \gtrsim 0.01$ higher twist contributions appear to be relevant (of the order of 10% at $Q^2 \simeq 1\,\mathrm{GeV}^2$) for $e(\mu)N$ data although they seem to be less pronounced in the corresponding νN measurements [46]. Our predictions for $xs(x, Q^2)$ are compared with the CCFR data [45], as extracted in LO from dimuon events, in Fig. 12. It should be noted that our theoretical results can be understood as absolute dynamical predictions throughout the whole x-region shown, since we have started with a vanishing strange sea input in (5) and (6), $xs(x, \mu^2_{\mathrm{LO,HO}}) = 0$. For illustration we also show our NLO result in Fig. 12 but refrain from comparing it with the corresponding CCFR data [51] since extracting $s(x, Q^2)$ in NLO is strongly model dependent. Our almost unique and perturbatively stable dynamical small-x predictions are finally compared in Fig. 13 with the most recent HERA F_2^{ep} data [8]. At the smallest values of Q^2 we also compare our predictions again with the available (preliminary) E665 data [50] which appear to confirm the very typical radiative (dynamical) predictions [3–5] that $F_2(x, Q^2)$ become *flat* at small-x for $Q^2 \simeq 1\,\mathrm{GeV}^2$.

For completeness we also show our predictions for $F_L(x, Q^2)$, as given in (14), in Fig. 14. This quantity plays an important role for extracting F_2 from cross section measurements $\mathrm{d}\sigma^{ep}/\mathrm{d}x\mathrm{d}Q^2$ in the small-x region as well as for extracting the gluon distribution from future measurements.

All our NLO calculations done so far refer to the $\overline{\mathrm{MS}}$ scheme. For completeness, we finally will also present our dynamical predictions for parton distributions in the occasionally used DIS factorization scheme [52, 41] although the resulting sea and gluon distributions do not

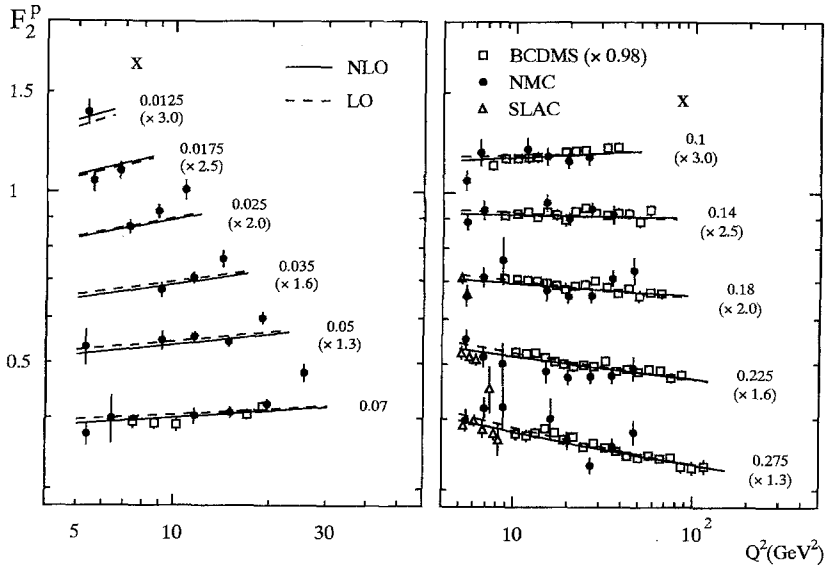

Fig. 10. Comparison of our LO and NLO fits to the fixed-target F_2^p data [17, 37, 39] in the medium-x and large Q^2 (≥ 5 GeV^2) region which were used for determining the valence-like gluon and sea inputs in (5) and (6). The charm contribution has always been calculated according to (12) for the LO process $\gamma^* g \to c\bar{c}$

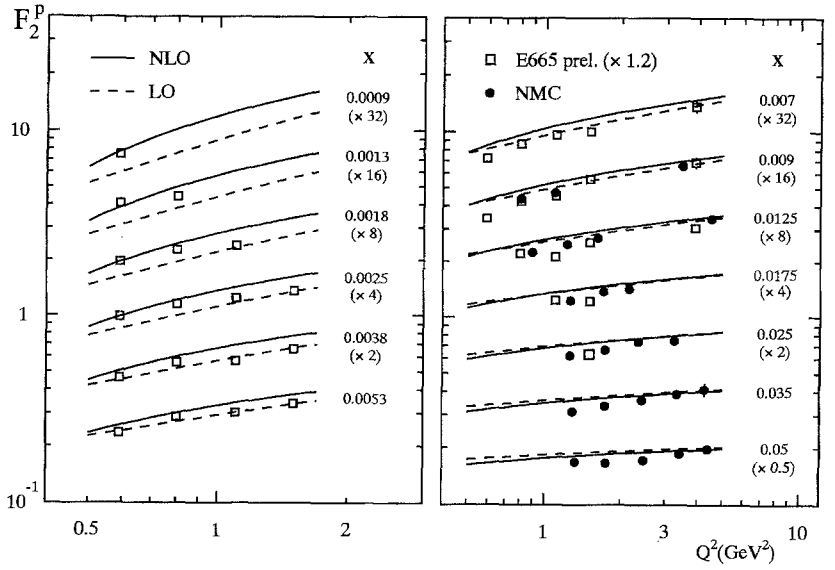

Fig. 11. Comparison of our LO and NLO small-x (leading-twist) predictions for F_2^p in (7) with the NMC [17] and preliminary E665 data [50] in the low-Q^2 region, $Q^2 < 5$ GeV^2

significantly differ [4] from the ones in the $\overline{\text{MS}}$ scheme throughout the relevant x-region, $x < 0.3$. In the DIS scheme the NLO($\overline{\text{MS}}$) light quark (u, d, s) and gluon contributions to F_2 in (7) are absorbed into the quark distributions by demanding that $F_2(x, Q^2)$ retains its LO form:

$$\frac{1}{x}F_2^{ep}(x,Q^2) = \sum_q e_q^2 \left[q_{\text{DIS}}(x,Q^2) + \bar{q}_{\text{DIS}}(x,Q^2)\right] + \frac{1}{x}F_2^c. \tag{19}$$

This, together with the energy momentum constraint ($n = 2$ Mellin moment),

$$\int_0^1 x\left[\sum_{q=u,d,s}(q(x,Q^2) + \bar{q}(x,Q^2)) + g(x,Q^2)\right]dx = 1, \tag{20}$$

can be satisfied by

$$\overset{(-)}{q}{}_{\text{DIS}}(x,Q^2) = \overset{(-)}{q}(x,Q^2) + \frac{\alpha_s(Q^2)}{2\pi}\left[C_{q,2}{}^* \overset{(-)}{q} + C_{g,2}{}^* g\right] + O(\alpha_s^2)$$

$$g_{\text{DIS}}(x,Q^2) = g(x,Q^2) - \frac{\alpha_s(Q^2)}{2\pi}\left[C_{q,2}{}^* \sum_{q=u,d,s}(q+\bar{q}) + 2fC_{g,2}{}^* g\right] + O(\alpha_s^2) \tag{21}$$

with $f = 3$. The transformation of the gluon distribution in (21) is the one conventionally chosen [52, 41] among the many possible solutions to the constraint (20) and is distinguished by being simple *and* smooth, i.e. analytic, in

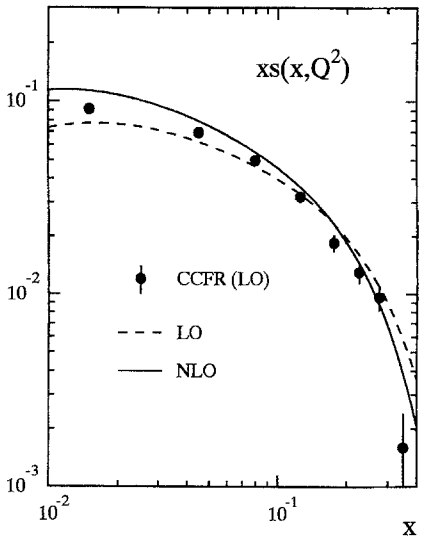

Fig. 12. Comparison of the radiative predictions for the strange sea distribution, starting from the vanishing input in (5) and (6), with the CCFR data [45], as extracted in LO from dimuon events. Errors are statistical only. Q^2 is approximately given, within 1%, by $Q^2(\mathrm{GeV}^2) = 154x\sqrt{1-x}$

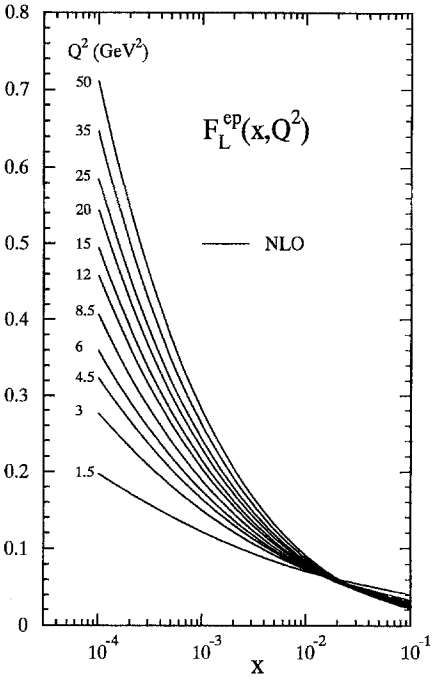

Fig. 14. Dynamical predictions for $F_L^{ep}(x, Q^2)$ according to (14)

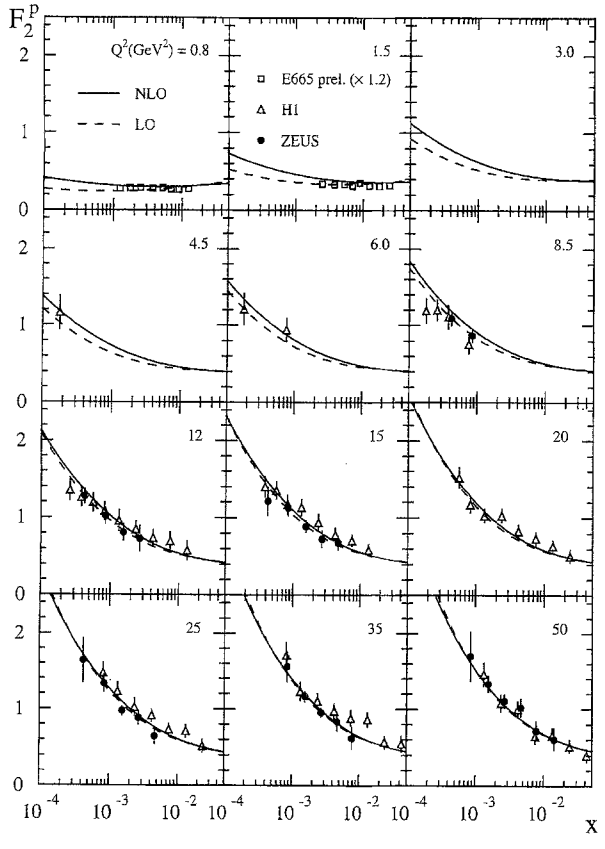

Fig. 13. Comparison of our radiative LO and NLO small-x predictions for F_2^p in (7) with recent HERA (H1, ZEUS) data [8] and with the preliminary E665 data [50] at small Q^2. The charm contribution has always been calculated according to (12) for the LO subprocess $\gamma^* g \to c\bar{c}$ and the marginal bottom-quark contribution has again been neglected

the Mellin n-moment space. Note that these transformations imply a corresponding change of the NLO splitting functions $P_{ij}^{(1)}$ as specified, e.g. in [41]. The parametrizations of the resulting DIS parton distributions are given in Appendix A.3.

4. Summary

Utilizing recent improved data at $x \gtrsim 10^{-2}$, we readjusted slightly our valence-like input distributions at a low resolution scale. The heavy quark contributions $(c, b, \ldots)$ to structure functions are treated by the perturbatively stable fixed-order perturbation theory for the relevant photon-parton fusion subprocesses. The resulting almost unique predictions of the radiatively generated (via LO and NLO renormalization group evolutions) parton distributions, being mainly due to the underlying QCD dynamics in the small-x region ($x \lesssim 10^{-2}$), are parametrized by simple analytic expressions in LO and NLO in the $\overline{\mathrm{MS}}$ as well as DIS factorization scheme. If the typical dynamical small-x predictions for sea and gluon distributions will continue to be in agreement with future measurements of structure functions, the fundamental twist-2 structure of nucleons appears indeed to be dominated by valence-like gluon and sea (current) quarks comoving with the valence current quarks at a low resolution scale of about 500–600 MeV, i.e. at a length scale of about 0.5 fm. These 'stuck-together' objects will eventually form the constituent quarks in the presently uncalculable *non*-perturbative region *below* 500 MeV (or at distances *larger* than 0.5 fm). This fundamental partonic structure appears to be universal and is very similar for mesons and photons as well as in the time-like region for fragmentation functions of hadrons and photons.

Acknowledgements. We thank H. Schellman for providing us with the preliminary E665 data tables and for discussions on their systematic uncertainties. This work has been supported in part by the 'Bundesministerium für Forschung und Technologie', Bonn.

Appendix

A.1 Parametrization of LO parton distributions

In order to obtain parametrizations of the radiative (dynamical) LO predictions valid for $Q^2 > \mu_{\rm LO}^2$ one has to generalize the simple ansatz for the input distributions in (5) as follows. Define

$$s \equiv \ln \frac{\ln [Q^2/(0.232\ \mathrm{GeV})^2]}{\ln [\mu_{\rm LO}^2/(0.232\ \mathrm{GeV})^2]} \tag{A.1}$$

to be evaluated for $\mu_{\rm LO}^2 = 0.23\ \mathrm{GeV}^2$. All following parametrizations are then valid for $0.4 \lesssim Q^2 \lesssim 10^6\ \mathrm{GeV}^2$ (i.e. $0.3 \lesssim s \lesssim 2.4$) and $10^{-5} \lesssim x < 1$. The non-singlet distributions can be parametrized as

$$xv(\mathrm{x}, Q^2) = Nx^a(1 + Ax^b + Bx + Cx^{3/2})(1-x)^D. \tag{A.2}$$

For $v = u_v$

$$\begin{aligned}
&a = 0.590 - 0.024s,\ b = 0.131 + 0.063s,\\
&N = 2.284 + 0.802s + 0.055s^2,\\
&A = -0.449 - 0.138s - 0.076s^2,\\
&B = 0.213 + 2.669s - 0.728s^2,\\
&C = 8.854 - 9.135s + 1.979s^2,\\
&D = 2.997 + 0.753s - 0.076s^2,
\end{aligned} \tag{A.3}$$

for $v = d_v$

$$\begin{aligned}
&a = 0.376,\ b = 0.486 + 0.062s,\\
&N = 0.371 + 0.083s + 0.039s^2,\\
&A = -0.509 + 3.310s - 1.248s^2,\\
&B = 12.41 - 10.52s + 2.267s^2,\\
&C = 6.373 - 6.208s + 1.418s^2,\\
&D = 3.691 + 0.799s - 0.071s^2,
\end{aligned} \tag{A.4}$$

and for $v = \Delta$

$$\begin{aligned}
&a = 0.409 - 0.005s,\ b = 0.799 + 0.071s,\\
&N = 0.082 + 0.014s + 0.008s^2,\\
&A = -38.07 + 36.13s - 0.656s^2,\\
&B = 90.31 - 74.15s + 7.645s^2,\\
&C = 0,\\
&D = 7.486 + 1.217s - 0.159s^2.
\end{aligned} \tag{A.5}$$

The gluon and sea $\bar{u} + \bar{d}$ distributions are parametrized as

$$\begin{aligned}
xw(x, Q^2) = \Bigg[& x^a(A + Bx + Cx^2)\left(\ln\frac{1}{x}\right)^b + s^\alpha \\
& \times \exp\left(-E + \sqrt{E' s^\beta \ln\frac{1}{x}} \right) \Bigg] (1-x)^D.
\end{aligned} \tag{A.6}$$

For $w = g$

$$\begin{aligned}
&\alpha = 0.524,\quad \beta = 1.088,\\
&a = 1.742 - 0.930s,\quad b = -0.399s^2,\\
&A = 7.486 - 2.185s,\\
&B = 16.69 - 22.74s + 5.779s^2,\\
&C = -25.59 + 29.71s - 7.296s^2,\\
&D = 2.792 + 2.215s + 0.422s^2 - 0.104s^3,\\
&E = 0.807 + 2.005s,\quad E' = 3.841 + 0.316s,
\end{aligned} \tag{A.7}$$

and for $w = \bar{u} + \bar{d}$

$$\begin{aligned}
&\alpha = 1.451,\quad \beta = 0.271,\\
&a = 0.410 - 0.232s,\quad b = 0.534 - 0.457s,\\
&A = 0.890 - 0.140s,\quad B = -0.981,\\
&C = 0.320 + 0.683s,\\
&D = 4.752 + 1.164s + 0.286s^2,\\
&E = 4.119 + 1.713s,\quad E' = 0.682 + 2.978s.
\end{aligned} \tag{A.8}$$

The strange sea distribution is parametrized as

$$\begin{aligned}
xw'(x, Q^2) = & \frac{s^\alpha}{(\ln\frac{1}{x})^a}\left(1 + A\sqrt{x} + Bx\right)(1-x)^D \\
& \times \exp\left(-E + \sqrt{E' s^\beta \ln\tfrac{1}{x}} \right)
\end{aligned} \tag{A.9}$$

i.e. for $w' = s = \bar{s}$

$$\begin{aligned}
&\alpha = 0.914,\quad \beta = 0.577,\\
&a = 1.798 - 0.596s,\\
&A = -5.548 + 3.669\sqrt{s} - 0.616s,\\
&B = 18.92 - 16.73\sqrt{s} + 5.168s,\\
&D = 6.379 - 0.350s + 0.142s^2,\\
&E = 3.981 + 1.638s,\quad E' = 6.402.
\end{aligned} \tag{A.10}$$

The contributions of heavy quarks ($h = c, b, \ldots$), being not an intrinsic part of the proton, should be calculated via (12) which derives from the $\gamma^* g \to h\bar{h}$ fusion subprocess. Rough estimates (valid to within a factor of 2-3, say) of heavy quark effects can be easier obtained, also for more involved subprocesses, with the help of the massless 'heavy' quark distributions $c(x, Q^2)$ and $b(x, Q^2)$ given in [4].

A.2 Parametrizations of NLO($\overline{MS}$) *parton distributions*

In order to obtain parametrizations of the radiative (dynamical) NLO predictions in the $\overline{\text{MS}}$ scheme which are valid for $Q^2 > \mu^2_{\text{HO}}$ one has to generalize the simple ansatz for the input distributions in (6) as done in the LO case. Define

$$s \equiv \ln \frac{\ln[Q^2/(0.248\ \text{GeV})^2]}{\ln[\mu^2_{\text{HO}}/(0.248\ \text{GeV})^2]} \tag{A.11}$$

to be evaluated for $\mu^2_{\text{HO}} = 0.34\ \text{GeV}^2$. All following parametrizations are then valid for $0.4 \lesssim Q^2 \lesssim 10^6\ \text{GeV}^2$ (i.e. $0.1 \lesssim s \lesssim 2.3$) and $10^{-5} \lesssim x < 1$. The non-singlet distributions are parametrized as in (A.2) where for $v = u_v$

$$a = 0.558 - 0.020s, \quad b = 0.183s,$$
$$N = 1.304 + 0.863s,$$
$$A = -0.113 + 0.283s - 0.321s^2,$$
$$B = 6.843 - 5.089s + 2.647s^2 - 0.527s^3,$$
$$C = 7.771 - 10.09s + 2.630s^2,$$
$$D = 3.315 + 1.145s - 0.583s^2 + 0.154s^3, \tag{A.12}$$

for $v = d_v$

$$a = 0.270 - 0.019s, \quad b = 0.260,$$
$$N = 0.102 - 0.017s + 0.005s^2,$$
$$A = 2.393 + 6.228s - 0.881s^2,$$
$$B = 46.06 + 4.673s - 14.98s^2 + 1.331s^3,$$
$$C = 17.83 - 53.47s + 21.24s^2,$$
$$D = 4.081 + 0.976s - 0.485s^2 + 0.152s^3, \tag{A.13}$$

and for $v = \Delta$

$$a = 0.409 - 0.007s, \quad b = 0.782 + 0.082s,$$
$$N = 0.070 + 0.042s - 0.011s^2 + 0.004s^3,$$
$$A = -29.65 + 26.49s + 5.429s^2,$$
$$B = 90.20 - 74.97s + 4.526s^2,$$
$$C = 0,$$
$$D = 8.122 + 2.120s - 1.088s^2 + 0.231s^3. \tag{A.14}$$

The gluon and sea distributions are parametrized as in (A.6) where for $w = g$

$$\alpha = 1.014, \quad \beta = 1.738$$
$$a = 1.724 + 0.157s, \quad b = 0.800 + 1.016s,$$
$$A = 7.517 - 2.547s,$$
$$B = 34.09 - 52.21\sqrt{s} + 17.47s,$$
$$C = 4.039 + 1.491s, \quad D = 3.404 + 0.830s,$$
$$E = -1.112 + 3.438s - 0.302s^2,$$
$$E' = 3.256 - 0.436s, \tag{A.15}$$

for $w = \bar{u} + \bar{d}$

$$\alpha = 0.877, \quad \beta = 0.561,$$
$$a = 0.275, \quad b = 0,$$
$$A = 0.997, \quad B = 3.210 - 1.866s,$$
$$C = 7.300,$$
$$D = 9.010 + 0.896\sqrt{s} + 0.222s^2,$$
$$E = 3.077 + 1.466s,$$
$$E' = 3.173 - 2.445\sqrt{s} + 2.207s, \tag{A.16}$$

and for $w' = s = \bar{s}$ in (A.9)

$$\alpha = 0.756, \quad \beta = 0.216,$$
$$a = 1.690 + 0.650\sqrt{s} - 0.922s,$$
$$A = -4.329 + 1.131s, \quad B = 9.568 - 1.744s,$$
$$D = 9.377 + 1.088\sqrt{s} - 1.320s + 0.130s^2,$$
$$E = 3.031 + 1.639s, \quad E' = 5.837 + 0.815s. \tag{A.17}$$

The contributions of heavy quarks ($h = c, b, \ldots$), being not an intrinsic part of the proton, derive from the appropriate photon-parton fusion subprocesses as calculated in NLO fixed order perturbation theory [15, 16]. Since the quantitative NLO analysis is very cumbersome and time consuming one can, for the time being, for all practical purposes use the much simpler LO expression in (12) as discussed in Sect. 3 and used throughout in this paper. For more general situations and processes, where the appropriate massive NLO subprocesses have not yet been calculated, a rough estimate of production rates involving heavy quarks can be easily obtained with the help of the NLO massless 'heavy' quark distributions $c(x, Q^2)$ and $b(x, Q^2)$ given in [4].

A.3. Parametrization of NLO(DIS) Parton Distributions

In order to obtain parametrizations of the radiative (dynamical) NLO predictions as calculated in the $\overline{MS}$ scheme but transformed to the DIS factorization scheme according to (21) we use the same analytic expressions as in (A.2) and (A.6) with s being given by (A.11). All following parametrizations are again valid for $0.4 \lesssim Q^2 \lesssim 10^6\ \text{GeV}^2$ and $10^{-5} \lesssim x < 1$. The valence distributions are parametrized as in (A.2) where for $v = u_v$

$$a = 0.563 - 0.025s, \quad b = 0.054 + 0.154s$$
$$N = 2.484 + 0.116s + 0.093s^2$$
$$A = -0.326 - 0.058s - 0.135s^2$$
$$B = -3.322 + 8.259s - 3.119s^2 + 0.291s^3$$
$$C = 11.52 - 12.99s + 3.161s^2$$
$$D = 2.808 + 1.400s - 0.557s^2 + 0.119s^3 \tag{A.18}$$

for $v = d_v$

$$a = 0.299 - 0.022s, \quad b = 0.259 - 0.015s$$

$$N = 0.156 - 0.017s,$$

$$A = 3.445 + 1.278s + 0.326s^2,$$

$$B = -6.934 + 37.45s - 18.95s^2 + 1.463s^3,$$

$$C = 55.45 - 69.92s + 20.78s^2$$

$$D = 3.577 + 1.441s - 0.683s^2 + 0.179s^3, \tag{A.19}$$

and for $v = \Delta$

$$a = 0.419 - 0.013s, \quad b = 1.064 - 0.038s$$

$$N = 0.099 + 0.019s + 0.002s^2,$$

$$A = -44.00 + 98.70s - 14.79s^2,$$

$$B = 28.59 - 40.94s - 13.66s^2 + 2.523s^3,$$

$$C = 84.57 - 108.8s + 31.52s^2,$$

$$D = 7.469 + 2.480s - 0.866s^2. \tag{A.20}$$

The gluon and light sea distributions are parametrized as in (A.6) where for $w = g$

$$\alpha = 1.258, \quad \beta = 1.846,$$

$$a = 2.423, \quad b = 2.427 + 1.311s - 0.153s^2,$$

$$A = 25.09 - 7.935s,$$

$$B = -14.84 - 124.3\sqrt{s} + 72.18s,$$

$$C = 590.3 - 173.8s, \quad D = 5.196 + 1.857s,$$

$$E = -1.648 + 3.988s - 0.432s^2,$$

$$E' = 3.232 - 0.542s, \tag{A.21}$$

for $w = \bar{u} + \bar{d}$

$$\alpha = 1.215, \quad \beta = 0.466,$$

$$a = 0.326 + 0.150s, \quad b = 0.956 + 0.405s,$$

$$A = 0.272, \quad B = 3.794 - 2.359\sqrt{s},$$

$$C = 2.014,$$

$$D = 7.941 + 0.534\sqrt{s} - 0.940s + 0.410s^2,$$

$$E = 3.049 + 1.597s,$$

$$E' = 4.396 - 4.594\sqrt{s} + 3.268s, \tag{A.22}$$

and for $w' = s = \bar{s}$ in (A.9)

$$\alpha = 0.175, \quad \beta = 0.344,$$

$$a = 1.415 - 0.641\sqrt{s},$$

$$A = 0.580 - 9.763\sqrt{s} + 6.795s - 0.558s^2,$$

$$B = 5.617 + 5.709\sqrt{s} - 3.972s,$$

$$D = 13.78 - 9.581s + 5.370s^2 - 0.996s^3,$$

$$E = 4.546 + 0.372s^2,$$

$$E' = 5.053 - 1.070s + 0.805s^2. \tag{A.23}$$

It should be noted that in certain kinematic regions (medium to large x and small Q^2) where gluon and sea distributions are negligibly small, the transformation (21) to the DIS scheme involves differences of small but almost equal terms which sometimes give rise to instabilities. Our parametrizations smoothly approach zero from above in these regions. In the relevant kinematic region ($x \lesssim 0.3$), as shown in [4], these DIS gluon and sea distributions are very similar to the ones in the $\overline{MS}$ scheme.

According to our specific parametrizations, the individual (anti) quark distributions are obviously given by

$$u = u_v + \bar{u}, \quad \bar{u} = \frac{1}{2}[(\bar{u} + \bar{d}) - \Delta]$$

$$d = d_v + \bar{d}, \quad \bar{d} = \frac{1}{2}[(\bar{u} + \bar{d}) + \Delta] .$$

A computer subroutine of our parametrizations is available upon request.

References

1. G. Parisi, R. Petronzio: Phys. Lett. 62B (1976) 331; V.A. Novikov, M.A. Shifman, A.I. Vainshtein, V.I. Zakharov: JETP Lett. 24 (1976) 341; Ann. Phys. (N.Y.) 105 (1977) 276; M. Glück, E. Reya: Nucl. Phys. B130 (1977) 76
2. M. Glück, R.M. Godbole, E. Reya: Z. Phys. C41 (1989) 667
3. M. Glück, E. Reya, A. Vogt: Z. Phys. C48 (1990) 471
4. M. Glück, E. Reya, A. Vogt: Z. Phys. C53 (1992) 127
5. M. Glück, E. Reya, A. Vogt: Phys. Lett. B306 (1993) 391
6. N.N. Nikolaev (Landau Inst., Moscow), Tokyo Univ. INS-Rep.-539 (1985), unpublished
7. S.J. Brodsky, I. Schmidt: Phys. Lett. B234 (1990) 144
8. I. Abt et al., H1 Collab.: Nucl. Phys. B407 (1993) 515; T. Ahmed et al., H1 Collab., DESY 95-006 (1995); M. Derrick et al., ZEUS Collab.: Phys. Lett. B316 (1993) 412; DESY 94-143 (1994)
9. I. Abt et al., H1 Collab.: Phys. Lett. B314 (1993) 436; M. Erdmann, Proceedings of the Workshop on Two-Photon Physics at LEP and HERA, Lund, May 1994, eds. G. Jarlskog, L. Jönsson (Lund Univ., 1994) p.71
10. J. Dainton (H1): AIP Conference Proceedings 302 of the XVI Int. Symposium on Lepton-Photon Interactions, Cornell Univ. Ithaca (NY 1993), eds. P. Drell and D. Rubin (AIP Press, New York, 1994) p. 87; J.F. Martin (ZEUS), ibid., p. 119; J. Feltesse, plenary talk presented at the 27th Int. Conf. on High Energy Physics, Glasgow, July 1994, Saclay DAPNIA/SPP 94-35
11. D.J. Miller: AIP Conference Proceedings 302 of the XVI. Int. Symposium on Lepton-Photon Interactions, Cornell Univ., Ithaca (NY 1993), eds. P. Drell, D. Rubin (AIP Press, New York, 1994) p. 654; experimental results presented in the Proceedings of the Workshop on Two-Photon Physics at LEP and HERA, Lund 1994, eds. G. Jarlskog and L. Jönsson (Lund Univ. press).
12. Proceedings of the Workshop 'HERA-the New Frontier for QCD' (Durham, March 1993), J. Phys. G: Nucl. Part. Phys. 19, No. 10 (1993) 1425–1703
13. M. Lüscher, R. Sommer, P. Weisz, U. Wolff: Nucl. Phys. B389 (1993) 247; Nucl. Phys. B413 (1994) 481; M. Lüscher, R. Narayanan, R. Sommer, P. Weisz and U. Wolff, Nucl. Phys. B (Proc. Suppl.) 30 (1993) 139
14. R.K. Ellis, Z. Kunszt, E.M. Levin: Nucl. Phys. B420 (1994) 517
15. M. Glück, E. Reya, M. Stratmann: Nucl. Phys. B422 (1994) 37
16. E. Laenen, S. Riemersma, J. Smith, W.L. van Neerven: Nucl. Phys. B392 (1993) 162

17. M. Arneodo et al., EM Collab.: Nucl. Phys. B333 (1990) 1; P. Amaudruz et al.: NM Collab., Phys. Lett. B295 (1992) 159
18. A.D. Martin, R.G. Roberts, W.J. Stirling: MRS (D'_0, D'_-): Phys. Lett. B306 (1993) 145; MRS(H): Rutherford Appleton Lab. RAL-93/077/Univ. Durham DTP/93/86; MRS(A): Phys. Rev. D50 (1994) 6734
19. M. Glück, E. Reya, A. Vogt: Nucl. Phys. B (Proc. Suppl.) 18C (1990) 49, and references therein
20. J. Botts et al. (CTEQ): Phys. Lett. B304 (1993)159
21. A. de Rujula, H. Georgi, H.D. Politzer: Ann. Phys. (N.Y.) 103 (1977) 315; Phys. Rev. D15 (1977) 2495
22. L.V. Gribov, E.M. Levin, M.G. Ryskin: Phys. Rep. 100 (1983) 1
23. A.H. Mueller, J. Qiu,: Nucl. Phys. B268 (1986) 427
24. D.J. Gross, F. Wilczek: Phys. Rev. D9 (1974) 980, and references therein; H.D. Politzer: Nucl. Phys. B172 (1980) 349; M. Okawa: Nucl. Phys. B172 (1980) 481; B187 (1981) 71; E.V. Shuryak, A.I. Vainshtein: Phys. Lett. B105 (1981) 65; R.K. Ellis, W. Furmanski, R. Petronzio: Nucl. Phys. B207 (1982) 1; B212 (1983) 29
25. M. Altmann, M. Glück, E. Reya: Phys. Lett. B285 (1992) 359
26. E.A. Kuraev, L.N. Lipatov, V. Fadin: JETP 44 (1976) 443; 45 (1977) 199; Ya.Ya. Balitzkij, L.N. Lipatov, Sov. J. Nucl. Phys. 28 (1978) 822; J.B. Bronzan. R.L. Sugar: Phys. Rev. D17 (1978) 585; T. Jaroszewicz: Phys. Lett. B116 (1982) 291; J. Kwiecinski: Z. Phys. C29 (1985) 561; J. Kwiecinski, A.D. Martin, W.J. Stirling, R.G. Roberts: Phys. Rev. D42 (1990) 3645; J. Bartels, M.G. Ryskin: Z. Phys. C60 (1993) 751
27. A.J. Askew, J. Kwiecinski, A.D. Martin, P.J. Sutton: Mod. Phys. Lett. A8 (1993) 3813; Phys. Rev. D49 (1994) 4402; N.N. Nikolaev and B.G. Zakharov: Phys. Lett. B327 (1994) 157; ibid. B328 (1994) 486
28. V.S. Fadin, L.N. Lipatov: Nucl. Phys. B406 (1993) 259
29. S. Catani, M. Ciafaloni, F. Hautmann: Phys. Lett. B242 (1990) 97; Nucl. Phys. B366 (1991) 135; Proceedings of the Workshop on "Physics at HERA", DESY, Hamburg, 1991, eds. W. Buchmüller and G. Ingelman, vol. 2, p. 690; J.C. Collins, R.K. Ellis: Nucl. Phys. B (Proc. Suppl.) 18C (1990) 80; Nucl. Phys. B360 (1991) 3
30. W.L. van Neerven, plenary talk on 'Higher Order QCD Corrections to Deep Inelastic Structure Functions' at the DESY Workshop '93 on QCD (DESY, Hamburg, 1993); E.B. Zijlstra, W.L. van Neerven: Nucl. Phys. B383 (1992) 525
31. A. Ukawa: Nucl. Phys. B (Proc. Suppl.) 30 (1993) 3, and references therein
32. M. Glück, E. Reya, A. Vogt: Z. Phys. C53 (1992) 651
33. M. Glück, E. Reya, A. Vogt: Phys. Rev. D45 (1992) 3986; D46 (1992) 1973
34. M. Glück, E. Reya, A. Vogt: Phys. Rev. D48 (1993) 116
35. M. Glück, L.E. Gordon, E. Reya, W. Vogelsang: Phys. Rev. Lett. 73 (1994) 388
36. P. Amaudruz et al., NM Collab.: Phys. Rev. Lett. 66 (1991) 2712
37. A.C. Benvenuti et al., BCDMS Collab.: Phys. Lett. B223 (1989) 485; ibid. B237 (1990) 592
38. A. Baldit et al., NA51 Collab.: Phys. Lett. B332 (1994) 244
39. L.W. Whitlow et al.: Nucl. Phys. B (Proc. Suppl.) 16 (1990) 215; Univ. Rochester report UR-1119 (1989); SLAC-report-357 (1990)
40. P. Aurenche et al.: Phys. Rev. D39 (1989) 3275
41. M. Diemoz, F. Ferroni, E. Longo, G. Martinelli: Z. Phys. C39 (1988) 21
42. M. Glück, E. Reya: Phys. Rev. D14 (1976) 3034
43. M. Glück, E. Reya: Phys. Lett. 69B (1977) 77; Phys. Rev. D16 (1977) 3242; I. Hinchliffe, C.H. Llewellyn Smith: Nucl. Phys. B128 (1977) 93
44. H. Abramowicz et al., CDHSW Collab.: Z. Phys. C15 (1982) 19
45. C. Foudas et al., CCFR Collab.: Phys. Rev. Lett. 64 (1990) 1207; S.A. Rabinowitz et al., CCFR Collab., ibid. 70 (1993) 134
46. Review of Particle Properties, Phys. Rev. D45 (1992) Part II, ibid. D50 (1994) 1173
47. S. Kretzer, E. Reya, M. Stratmann: Univ. Dortmund DO-TH 94/26 (Phys. Lett. B)
48. W.T. Giele, E.W.N. Glover, D. Kosower: Nucl. Phys. B403 (1993) 633
49. A. Bodek, CDF Collab.: Univ. Rochester report UR-1351, Proc. of the Internat Workshop on Deep Inelastic Scattering, Eilat, Israel, Feb. 1994; CDF Collab.: Fermilab-Conf-94/146-E, submitted to the 27th Internat. Conf. on High Energy Physics, Glasgow, July 1994; M. Dickson, CDF Collab.: Univ. Rochester report UR-1349 (1994), unpublished.
50. E665 Collab., A.V. Kotwal: Fermilab-Conf-94/345-E, presented at the VIth Rencontres de Blois, France, June 1994; H. Schellman, private communication, Sept. 1994; J. Feltesse, [10]
51. A.O. Bazarko et al., CCFR collab.: Columbia Univ. report NEVIS R#1502 (1994)
52. G. Altarelli, R.K. Ellis, G. Martinelli: Nucl. Phys. B143 (1978) 521; B146 (1978) 544(E); ibid. B157 (1979) 461